Cement and Concrete Research 39 (2009) 1149–1155

Contents lists available at ScienceDirect

Cement and Concrete Research

journal homepage: http://ees.elsevier.com/CEMCON/default.asp

Modeling of diffusive mass transport in micropores in cement based materials ☆

Tetsuji Yamaguchi [a,*], Kumi Negishi [a,b], Seiichi Hoshino [a], Tadao Tanaka [a]

[a] Japan Atomic Energy Agency, Shirakata, Tokai, Ibaraki 319-1195, Japan
[b] Taiheiyo Consultant Company Limited, 2-4-2, Osaku, Sakura, Chiba 285-8655, Japan

ARTICLE INFO

Article history:
Received 28 September 2008
Accepted 19 August 2009

Keywords:
Microstructure (B)
Diffusion (C)
Long-term performance (C)
Modeling (E)
Waste management (E)

ABSTRACT

In order to predict long-term leaching behavior of cement constituents for safety assessments of radioactive waste disposal, we modeled diffusive mass transport in micropores in cement based materials. Based on available knowledge on the pore structure, we developed a transport porosity model that enables us to estimate effective porosity available for diffusion (transport porosity) in cement based materials. We microscopically examined the pore structure of hardened cement pastes to partially verify the model. Effective diffusivities of tritiated water in hardened cement pastes were also obtained experimentally, and were shown to be proportional to the estimated transport porosity.

1. Introduction

High-level radioactive waste generated from reprocessing of spent nuclear fuel in Japan is vitrified, encapsulated in a metal container called overpack, surrounded by engineered buffer material, and emplaced in a deep geological repository. Cement based materials will be used as structural materials to support the disposal tunnels, and bentonite clay will be used as the engineered buffer material to reduce permeation of groundwater and migration of radionuclides. Over a long time period, cement based materials will be altered by contact with groundwater. Highly alkaline pore water will be leached from the cement based materials, and is likely to cause the physical properties such as hydraulic conductivity and/or chemical properties such as sorptivity of the buffer materials to deteriorate. In order to evaluate the alteration of bentonite, the leaching behavior of cement constituents should be modeled mathematically. Diffusion of solutes in cement based materials is the important factor that will determine the process of leaching of cement constituents. Therefore, we focus on modeling of diffusion of solutes in cement based materials in order to predict the long-term leaching behavior of cement constituents. Diffusion of dissolved chemical species in cement based materials is a combined process of physical transport and chemical interactions. The objective of this study is to model the physical transport in cement based materials.

In previous studies, the diffusivity of solutes in cement based materials has been of interest and modeled as a function of porosity. Numata et al. [1] reported the diffusivity of tritiated water in cement based materials as a function of the porosity obtained by mercury intrusion porosimetry:

$$D_e = 3.55 \times 10^{-11} \phi^{0.947}, \quad (1)$$

where D_e is the effective diffusivity of tritiated water in cement based materials, and ϕ is the porosity of cement based materials. Mihara et al. [2] proposed the diffusivity of tritiated water in cement based materials as the third power of the porosity:

$$D_e = D_v \phi^{3.05}, \quad (2)$$

where D_v is the diffusivity in free water. The two equations yield quite different estimates on the porosity value, which seems to attribute to a lack of information on the pore structure. Garboczi and Bentz [3] modeled the microstructure of hardened cement pastes by applying percolation theory and quantitatively explained the dependence of diffusivity of chloride ion in plain Portland cement paste with the following expression:

$$\frac{D_e}{D_v} = 0.001 + 0.07\phi_{cp}^2 + H\left(\phi_{cp} - 0.18\right) \times 1.8 \times \left(\phi_{cp} - 0.18\right)^2, \quad (3)$$

where ϕ_{cp} is the capillary porosity of cement based materials, H the Heaviside's step function of $H(x) = 0$ for $x \leq 0$, and 1 for $x > 0$. Modeling the diffusivity in cement based materials needs scientific soundness, therefore should be based on reliable information on the pore structure.

In this study, based on available knowledge on the structure of micropores in cement based materials, we developed a transport porosity model that enables us to estimate effective porosity available for diffusion. We analyzed the micropores of hardened cement pastes

☆ This is a part of a study funded by the Nuclear and Industrial Safety Agency, Ministry of Economy, Trade and Industry, Japan.

* Correspondent author. Japan Atomic Energy Agency, Shirakata, Tokai, Ibaraki 319-1195, Japan
E-mail address: yamaguchi.tetsuji@jaea.go.jp (T. Yamaguchi).

0008-8846/$ – see front matter © 2009 Elsevier Ltd. All rights reserved.
doi:10.1016/j.cemconres.2009.08.012

by image analysis to partially verify the transport porosity model. We used non-sorbing tritiated water in order to investigate the physical transport process independently of the chemical interactions. We also determined the effective diffusivity of tritiated water in the hardened cement pastes to establish the correlation between the transport porosity and the effective diffusivity and discussed validity of the correlation.

2. Development of a transport porosity model

2.1. Basic concepts

The pore spaces of various size are known to be present in cement based materials [4]. The pore spaces in hardened cement paste, mortar, and concrete consist of air and water voids. The air void includes the entrapped air rolled up during the mixing process and the entrained air with air-entraining agents. The water voids are comprised of the gel pore space corresponding to the space between the C–S–H interlayer and capillary pore space unfilled with the hydrated minerals in hardened specimens [4]. Part of the pore space is not effective for the diffusive transport. Goto et al.[5] reported that the diffusivity in hardened cement is not correlated with the total porosity but negatively correlated with the partial porosity of the pores with the diameter below 2 nm. They presumed that the diffusivity was dominated by the connected pores of relatively large size, which decreased with the increase in the smaller pores. Atkinson and Nickerson [6] measured diffusion-related parameters for several ions in cement pastes to identify mechanisms of the diffusion. They concluded that the results could not be rationalized by the simple pore-diffusion model and that each ion had more than one diffusion processes in the cement, which were characterized as fast and slow diffusivity networks in the cement pore space. These studies did not identify the pore space dominating the diffusive transport although empirically discussed the correlations between the diffusivity and the pore structure. It is necessary to identify and quantify the pore space dominating the diffusive transport.

Nishiyama et al. [7] studied the correlation between effective diffusivity of iodide anion (I^-) and the porosity in rocks. They classified the pores into transport and storage pores according to diameters of the pores. They successfully correlated the effective diffusivity of I^- in rocks to the transport porosity and explained quantitatively the effective diffusivity in accordance with the pore-diffusion model. Our model intends to categorize the pores in cement based materials by the transport properties and to quantify the porosity which effectively acts as diffusive transport paths.

The air voids are dispersed in the cement based materials and do not form effective transport paths by being interconnected each other. Therefore, we assume that the air voids act as storage pores, not the transport pores ignoring moisture transport. The gel pores are also assumed not to act as the transport paths, because almost all the water filling the gel pore space is confined in the C–S–H interlayer [8]. These assumptions may be valid only for pastes with high w/c ratio; gel pores are in charge of slow transport process for pastes with w/c ratio lower than 0.38. The capillary pores are the residual space unfilled with hydrated cement minerals after the hydration process as shown schematically in Fig. 1. It is inferred from the formation process that the capillary pores have large variety in size and those with relatively large size are connected via those with smaller size. We assume that a part of capillary pores with small sizes are self-connected pores and can be act as transport pore. This is called capillary transport pore. The other part of the capillary pores with larger size is assumed to act as storage pore space and is called capillary storage pore.

Transport porosity which counts the capillary transport pores forming diffusion paths in cement based materials is expressed as

$$\phi_{tra} = V_{cp-tra} / V_{tot}, \tag{4}$$

where $V_{cp\text{-}tra}$ is the volume of capillary transport pores and V_{tot} the total volume of the hardened cement based materials. It is necessary to determine $V_{cp\text{-}tra}$ and V_{tot} to estimate the transport porosity.

2.2. Model for evaluating porosities in cement based materials

(1) Total volume of the hardened cement based materials
The volume distribution of the minerals and pores is calculated based on the model of Powers and Brownyard [9]. The total volume of a cement based material is calculated by summing up volumes of the original cement, water, aggregates and air void as

$$V_{tot} = V_w + V_c + V_{fa} + V_{ca} + V_a, \tag{5}$$

where V_w is the volume of original water, V_c the volume of original cement, V_{fa} the volume of fine aggregates, V_{ca} the volume of coarse aggregate and V_a the volume of air void. The volume of original water is supplemented with volume of absorbed water during the curing process which is approximately 6% [10] of the original cement in weight. This value is assumed based on the knowledge on the hydration of ordinary Portland cement with w/c ratio between 0.38 and 0.8 [10].

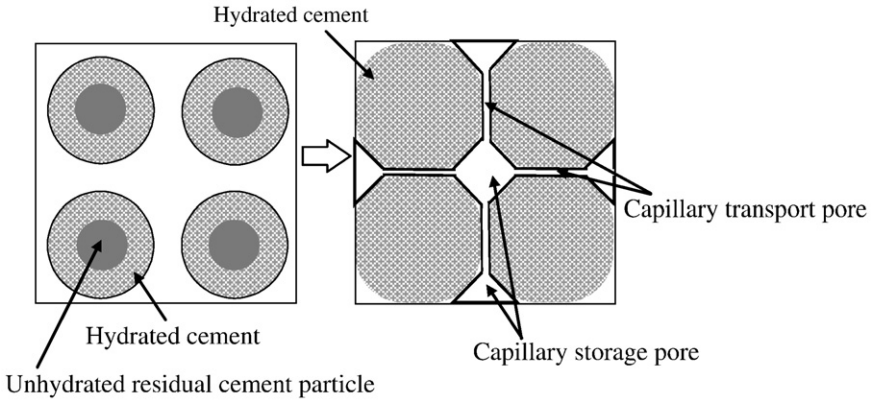

Fig. 1. Schematics of formation of capillary storage pore and capillary transport pore accompanied by hydration of cement particles. Capillary pore is the residual space unfilled with the hydrated cement after the hydration process. The capillary pores with relatively larger sizes (capillary storage pores) are connected through the smaller ones (capillary transport pores).

Powers suggested that cement minerals can be fully hydrated at the water to cement ratio (w/c) of 0.38 or higher [9]. Our model treated cement based materials as fully cured ones with sufficient supply of water and ignored the volume of pores in unhydrated cement minerals in Eq. (5). Applicability of our model is limited to the w/c higher than 0.38. Cement minerals are not fully hydrated at lower w/c, for example, 69% hydrated at w/c of 0.25 after 91 days of curing [11].

(2) The volume of capillary pores
The volume of the capillary pores, V_{cp}, is estimated by subtracting volumes of the cement hydrates, fine aggregates, coarse aggregates and air void from V_{tot}.

$$V_{cp} = V_{tot} - V_{hyd} - V_{fa} - V_{ca} - V_a, \quad (6)$$

where V_{hyd} is the volume of cement hydrate. V_{hyd} can be estimated to be 2.2 V_c [10].

(3) Volumes of the capillary transport pores
The volume of the capillary transport pores, $V_{cp\text{-}tra}$ is estimated by subtracting $V_{cp\text{-}sto}$ from V_{cp}:

$$V_{cp-tra} = V_{cp} - V_{cp-sto}, \quad (7)$$

where $V_{cp\text{-}sto}$ is the volume of capillary storage pores.

2.3. Estimating the volume of the capillary storage pores

Volumes of the capillary storage pores and the capillary transport pores in hardened cement paste shown in Fig. 1 vary with w/c. The relationship of the capillary pores in hardened cement pastes and the w/c is schematically shown in Fig. 2. At low w/c, both of $V_{cp\text{-}sto}$ and $V_{cp\text{-}tra}$ increase as the V_{cp} increases. We assumed proportionality between V_{cp} and $V_{cp\text{-}sto}$ at low w/c. At high w/c, the increase in V_{cp} enhances connectivity of the capillary pores, increases the $V_{cp\text{-}tra}$, and does not increase the $V_{cp\text{-}sto}$ any more. The limiting w/c value is set at 0.57, which is the volume ratio between spherical particles and voids in the closest packing. The volume of the capillary storage pores is given by

$$V_{cp-sto} = mV_{cp} \quad 0.38 < w/c \le 0.57 \quad (8)$$

and

$$V_{cp-sto} = mV_{cp\,|\,w/c=0.57} \quad 0.57 < w/c, \quad (9)$$

where m is a constant representing the proportion of capillary storage pores to the capillary pores.

The size of the capillary pores ranges from 10 nm to several tens micrometers [4]. Diamond and Leeman [12] determined pore size distribution of hardened cement paste by image analysis with scanning electron microscope (SEM) and mercury intrusion porosimetry (MIP). They observed capillary pores in the diameter range smaller than 0.2 μm by MIP. On the other hand, they observed capillary pores with a diameter range of 1–10 μm by SEM (Fig. 3). The reason why MIP did not observe the capillary pores with a diameter range of 1–10 μm arise from the pore structure of hardened cement paste. The MIP determined the pore size distribution by forcing mercury into the pores. For ink-bottle-type pores, MIP determined the diameter of the bottleneck instead of the actual diameter of the main

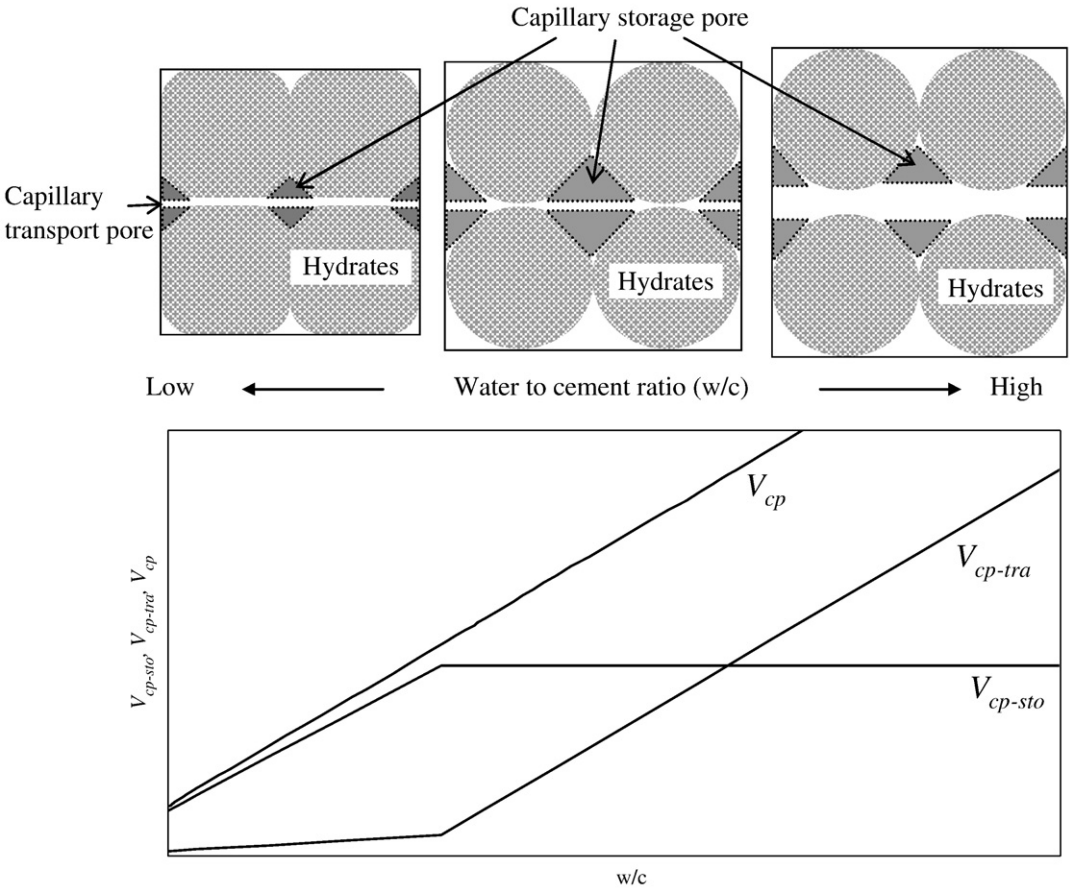

Fig. 2. Conceptual image of the capillary pores in hardened cement pastes for different water to cement ratios (upper), and dependence of volumes of capillary storage pore, capillary transport pore and capillary pore on w/c.

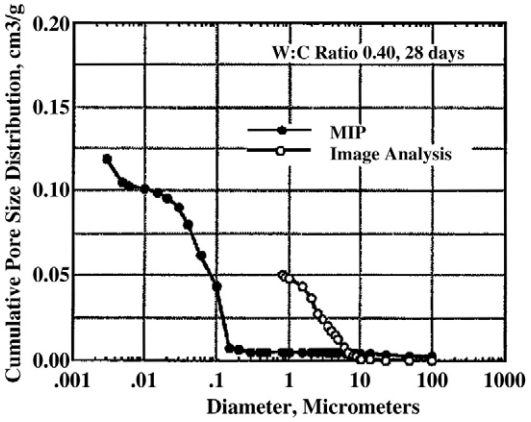

Fig. 3. Pore size distribution of a hardened cement paste obtained by image analysis and mercury intrusion porosimetry (MIP) [12]. The difference in pore size distribution for the same sample with different analytical methods arises from the pore structure of hardened cement paste where the capillary storage pores with larger sizes are interconnected with the capillary transport pores with smaller sizes.

pore space. Capillary pores with a diameter range of 1–10 μm are present in the hardened cement paste as indicated by the SEM image analysis. They are not directly interconnected each other, but are interconnected with the capillary pores whose diameter is smaller than 0.2 μm as observed by MIP. In other words, the diameter of the capillary transport pores is smaller than 0.2 μm. The SEM image analysis gives us information on actual size and volume of the capillary pores and does not count the volume of the capillary transport pores because of the detection limit, which was 0.8 μm in the SEM image analysis performed by Diamond and Leeman [12]. We, therefore, assumed that the pore volume observed by the image analysis correspond to the volume of capillary storage pores. Diamond and Leeman [12] determined the porosity of a 28 days cured hardened cement paste with a w/c of 0.4 to be 0.094 through image analysis. The value was taken as the capillary storage porosity in this study. The capillary porosity of the specimen was estimated by Eqs. (5) and (6) to be 0.102. The constant, m, was determined by Eq. (8) to be 0.9.

3. Experiments

We analyzed the pore structure of hardened cement paste specimens to verify our transport porosity model. We also determined effective diffusivity of tritiated water by through-diffusion experiments for the hardened cement paste specimens to find the correlation between D_e and ϕ_{tra}.

3.1. Image analysis

The cement paste specimens were prepared from ordinary Portland cement (OPC). Chemical compositions of the OPC used in the tests are shown in the Table 1. OPC was mixed with deionized water at w/c of 0.45, 0.6 and 0.75 by weight.

The hardened cement pastes were cured at 50 °C under deionized water for 45 days until the XRD peaks for unhydrated cement disappear and cut into cylindrical specimens of 30 mmϕ × 10 mmt. The specimens were vacuum-dried and embedded in epoxy resin. The epoxy resin was cut into two pieces and the specimen surfaces were polished. The polished surfaces were applied for the image analysis.

The image analysis was carried out using a digital microscope (KH-3000 V, Hirox, Tokyo). The image taken at the magnification of 3500 was optimized to provide sharp and clear boundaries between solid and pore space. The optimized image file was modified by binary segmentation process using Adobe Photoshop 5.0 J. The dark portion in the images is regarded as the capillary storage pore and the area was determined by calculating the pixels. The capillary storage porosity is the ratio of the area of the dark portion to that of the whole surface. A hundred images were processed for each specimen to determine the capillary storage porosity. The minimum size of the capillary storage pores detected in the image analysis was 0.12 μm.

Table 1
Chemical compositions of OPC used in the experiment (wt.%).

SiO_2	CaO	Al_2O_3	Fe_2O_3	MgO	SO_3	Na_2O	K_2O
21.0	63.7	5.9	3.0	1.3	2.5	0.2	0.3

3.2. Diffusion of tritiated water

The diffusivity of tritiated water in the cylindrical hardened cement paste was determined by the through-diffusion method using acrylic diffusion cell. The acrylic diffusion cells used in this study are shown in Fig. 4. The procedure for preparing the 30 mmϕ 10 mmt hardened cement paste was identical with those of image analysis. The cylindrical hardened cement paste specimen was sealed into an acrylic partition using silicon-based sealant. The working solution was 1.5 mol dm^{-3} $NaClO_4$ solution whose pH was adjusted to 11 with a NaOH solution. The sealed specimens were soaked in the working solution under vacuum to evacuate air from the pores in the specimens. The diffusion cell was assembled and was transferred into a controlled atmosphere glove box filled with argon to eliminate carbonation of hardened cement paste. Two reservoirs were filled with the working solution and one of the reservoirs (referred to as "high-concentration reservoir") was spiked with tritiated water to get a concentration of 1.0×10^2 Bq cm^{-3}. One cubic centimeter of aliquot from the low-concentration reservoir and a 0.02 cm^3 aliquot from the high-concentration reservoir were taken to determine the concentration of tritiated water with liquid scintillation counter. Sampling intervals were 1 to 3 days. The 1 cm^3 aliquot removed from the low-concentration reservoir was replaced by an equal volume of the working solution to maintain the balance of water level between the two reservoirs. The through-diffusion runs were conducted in the

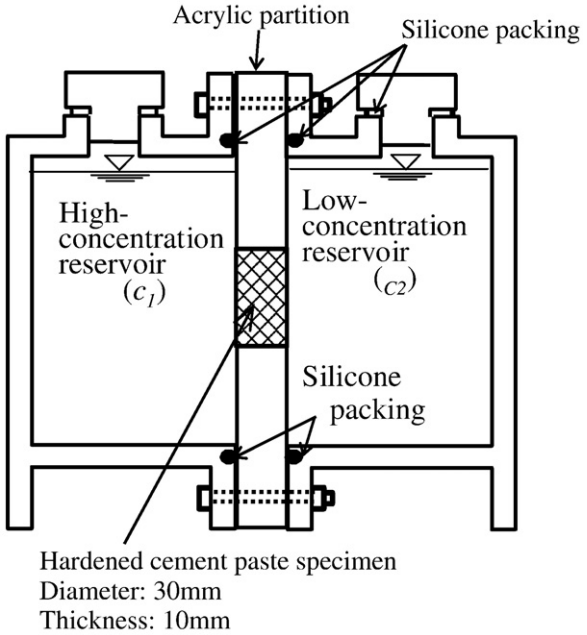

Fig. 4. Schematic drawing of the through-diffusion cell used in experiments.

glove box at room temperature (28 °C). The deviation of the diffusivity at 28 °C from that at 20 °C was about 25% and was ignored in this paper.

4. Result and discussion

4.1. Image analysis

The microscopic image of the hardened cement paste and the binarized one are shown in Fig. 5. The dark portion in the binarized image corresponds to the pores. Pores in the size range between a few and 10 μm are observed. We regarded the porosity determined by the image analysis as the capillary storage porosity, as discussed in Section 2.3. The capillary storage porosities determined by the image analysis and the capillary porosities estimated by using Eqs. (5) and (6) assuming that $V_a = 0$ are shown in Table 2. The capillary storage porosity determined by the image analysis for the specimen with w/c of 0.75 is lower than that of 0.60. This trend is consistent with our model in which the volume of the capillary storage pores does not increase with increasing w/c at the w/c ratio of 0.57 or higher as shown in Fig. 2, while the total volume of the specimen increases with w/c. The capillary storage porosity determined through our image analysis are plotted versus the capillary porosity in Fig. 6. It seems that our experimental values are closely plotted to the estimation by our $V_{cp\text{-}sto}-V_{cp}$ model. This result is indicative of validity of our transport porosity model although the validity of the model is based on only three experimental points.

4.2. Diffusion of tritiated water

The changes in the concentration of tritiated water with time in the diffusion experiments are shown in Fig. 7. The concentrations of tritiated water in the high-concentration reservoirs decrease and those in the low-concentration reservoirs increase with time. The increasing rates are identical to the decreasing rates as shown in Table 3, which ensures that the steady state flux of tritiated water was established in the cylindrical hardened cement paste. The effective diffusivity is evaluated using Eq. (10) based on the Fick's law:

$$J = -D_e \partial c / \partial x, \tag{10}$$

where J is the diffusive flux (Bq m^{-2} s^{-1}) and $\partial c/\partial x$ the concentration gradient (Bq m^{-4}). The diffusive flux was obtained from

$$J = (\Delta c_2 / \Delta t) V A^{-1}, \tag{11}$$

where $\Delta c_2/\Delta t$ is the rate of increase of the concentration of tritiated water (Bq m^{-3} s^{-1}), V the volume of the solution in the reservoir (1.1×10^{-4} m^3) and A the cross section of the hardened cement paste specimen (7.07×10^{-4} m^2). The value of $\Delta c_2/\Delta t$ was obtained from the slope of the liner portion of the through-diffusion curves shown in Fig. 7. The concentration gradient, $\partial c/\partial x$, was obtained from a difference in the concentrations of tritiated water in the two reservoirs as

$$\partial c / \partial x = (\overline{c_1} - \overline{c_2}) L^{-1}, \tag{12}$$

where L is the thickness of the specimens (0.01 m), $\overline{c_1}$ the average concentration of tritiated water in the high-concentration reservoir (Bq m^{-3}) and $\overline{c_2}$ the average concentration of tritiated water in the low-concentration reservoir (Bq m^{-3}). Effective diffusivities were obtained by combining Eqs. (10), (11) and (12) and are shown in Table 3. Errors associated with the evaluation of the average concentration in Eq. (12) induced errors of 7–13% to the evaluation of the effective diffusivity. The effective diffusivities are plotted in Fig. 8 versus the transport porosity estimated by Eqs. (4)–(9) together

Table 2
Porosity of hardened cement paste.

w/c	Capillary storage porosity by the image analysis	Capillary porosity by Eq. (5)
0.45	0.134 ± 0.006	0.16
0.6	0.224 ± 0.014	0.29
0.75	0.189 ± 0.011	0.38

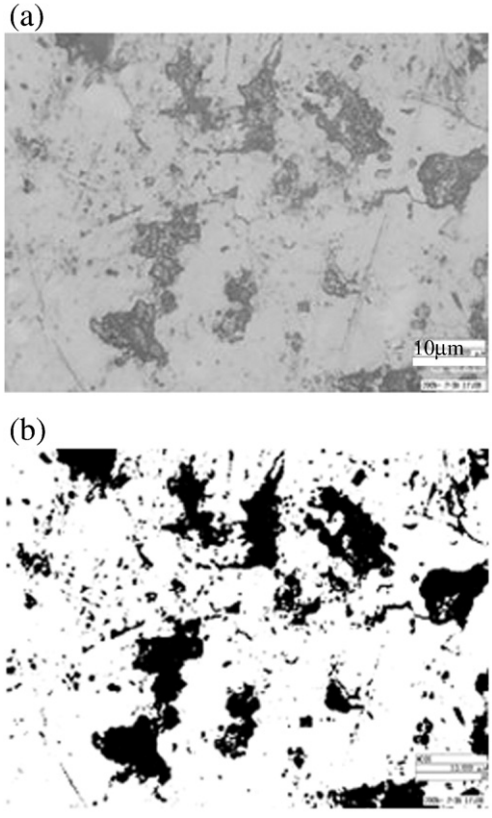

Fig. 5. A microscopic image of hardened cement paste with w/c of 0.6 (a). A binary segmentation was performed to obtain the image (b) showing the pore space pixels as black and solid material pixels as fully white.

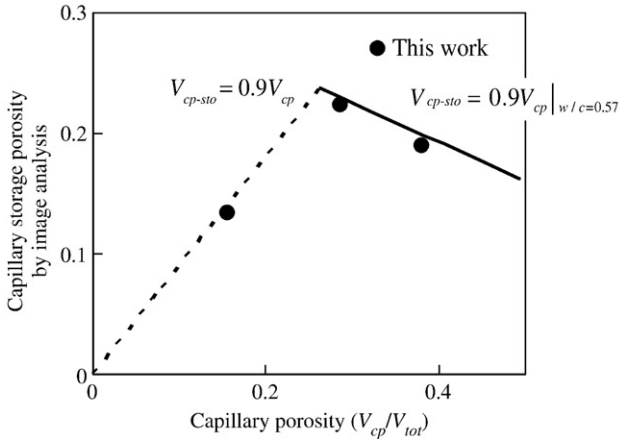

Fig. 6. Capillary storage porosity determined by image analysis versus capillary porosity estimated by Eq. (5). The broken and the solid lines represent the estimation by the model, Eqs. (8) and (9), respectively.

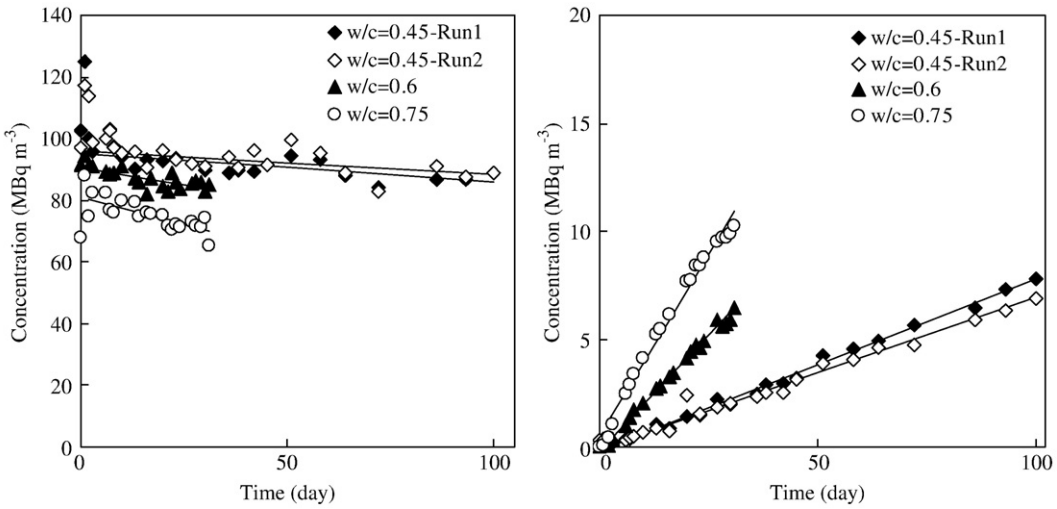

Fig. 7. Concentrations of tritium in solutions in the high-concentration reservoirs (left) and those in low-concentration reservoirs (right).

with literature data [1,13,14]. The effective diffusivities fall in a line on the logarithmic plot and can be approximated by

$$D_e = 4.16 \times 10^{-10} \phi_{tra}^{0.94}, \quad (13)$$

although the diffusivity can be varied with temperature and the conditions of curing [15]. The data can also be expressed as the following equation because the slope of the plot, 0.94 ± 0.08, is virtually unity.

$$D_e = 5.37 \times 10^{-10} \phi_{tra}^{1.0}, \quad (14)$$

Diffusion of solutes in constrained geometry of a porous medium is often interpreted by applying the pore-diffusion model:

$$D_e = D_v \phi \frac{\delta}{\tau^2}, \quad (15)$$

where D_e is the effective diffusivity of solutes in the medium, D_v the diffusivity in free water, ϕ; the porosity of porous medium, δ the constrictivity and τ the tortuosity [16]. The constrictivity (0.4 to 1.0 [16]) accounts for that the cross section of a pore space varies over its length. The tortuosity accounts for that the main diffusion paths are not parallel to the concentration gradient and takes a value between 1 and $\sqrt{3}$ depending on the porosity [16]. D_v is the self-diffusion coefficient of tritiated water in free water (2.3×10^{-9} m^2 s^{-1} at 28 °C [17]). Thus, the $D_v \delta \tau^{-2}$ must range between 3.0×10^{-10} and 2.3×10^{-9}. The proportional constant of Eq. (14), $D_v \delta \tau^{-2}$, of 5.37×10^{-10} falls within the range. We successfully demonstrated that the "pore" of the "pore-diffusion model" should be understood as "transport pore" for the mass transport in cement based materials, and that the transport can be described by the "transport pore-diffusion" model.

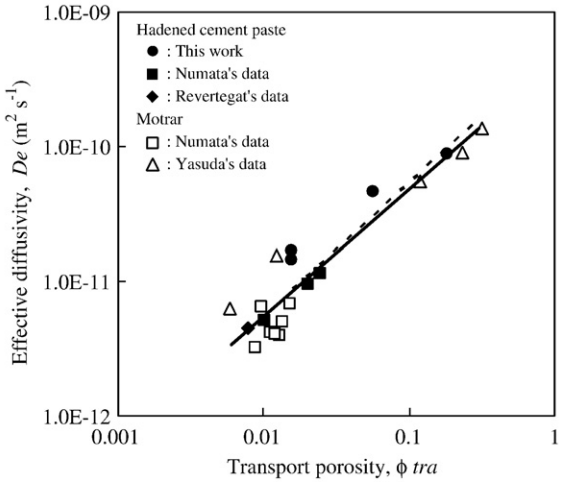

Fig. 8. Effective diffusivity, D_e, as a function of transport porosity, ϕ_{tra}. The least squares fitting gives $D_e = 4.16 \times 10^{-10} \phi_{tra}^{0.94}$ (solid line) and $D_e = 5.37 \times 10^{-10} \phi_{tra}$ (broken line) where the slope was fixed at 1.0. The correlation coefficient was 0.88 for either of the fittings.

Table 3
Effective diffusivity of tritium in hardened cement paste.

w/c	Diffusive flux of tritium (Bq m^{-2} s^{-1})		Effective diffusivity, D_e (m^2 s^{-1})
	From decreasing rate of c_1 (high-concentration reservoir)	From increasing rate of c_2 (low-concentration reservoir)	
0.45-Run1	0.17 ± 0.08	0.144 ± 0.005	$(1.66 \pm 0.13) \times 10^{-11}$
0.45-Run2	0.14 ± 0.11	0.126 ± 0.005	$(1.43 \pm 0.11) \times 10^{-11}$
0.6	0.38 ± 0.19	0.383 ± 0.015	$(4.59 \pm 0.32) \times 10^{-11}$
0.75	0.63 ± 0.25	0.601 ± 0.039	$(8.7 \pm 1.1) \times 10^{-11}$

The present transport porosity model contributes to reliable assessment of diffusivity of solutes in cement based materials for performance assessments of engineered barrier system in high-level radioactive waste disposal.

5. Conclusion

We developed a transport porosity model for cement based materials. We categorized the pore space of cement based materials into the storage pore and the transport pore to quantify the dominant diffusion paths. Our model quantifies the capillary transport pores that are effective for diffusion. We examined the pore structure of hardened cement pastes by the microscopic image analysis to partially verify the model. We confirmed that the diffusivity of tritiated water in cement based materials can be correlated with the transport porosity consistent with previously acknowledged pore-diffusion model.

Acknowledgements

Mr. M. Tsukada of Nuclear Engineering Co. and Mr. Y. Ootani of Kanazawa University (present affiliation: Shuhou Mining Co. Ltd.) are acknowledged for their contribution to the experiments.

References

[1] S. Numata, H. Amano, K. Minami, Diffusion of tritiated water in cement materials, J. Nucl. Mater. 171 (1990) 373–380.
[2] M. Mihara, R. Sasaki, RAdio-nuclides Migration DAtasets(RAMDA) on cement, bentonite and rock for the performance assesment of TRU waste repository in Japan, JNC TN 8400 2005-027 (2005) pp. 10–13.
[3] E.J. Garboczi, D.P. Bentz, Computer simulation of the diffusivity of cement-based materials, J. Mater. Sci. 27 (1992) 2083–2092.
[4] H. Uchikawa, S. Uchida, S. Hanehara, Measuring method of pore structure in hardened cement paste, mortar and concrete, il cemento 2 (1991) 67–90.
[5] S. Goto, H. Shigeru, T. Takagi, M. Daimon, JCA Review of the 36th General Meeting, 1982, pp. 49–52, (in Japanese).
[6] A. Atkinson, A.K. Nickerson, Diffusion and sorption of cesium, strontium, and iodine in water-saturated cement, Nucl. Technol. 81 (1988) 100–113.
[7] K. Nishiyama, S. Nakashima, R. Tada, T. Uchida, Diffusion of an ion in rock pore water and its relation to pore characteristics, Mining Geol. (in Japanese) 40 (1990) 323–336.
[8] M. Daimon, S.A. Abo-El-Enein, G. Hosaka, S. Goto, R. Kondo, Pore structure of calcium silicate hydrate in hydrated tricalcium silicate, J. Am. Ceram. Soc. 60 (1977) 110–114.
[9] T.C. Powers, T.L. Brownyard, Studies of the physical properties of hardened cement paste, J. Am. Concr. Inst. 43 (1947) 249–336, 469–504, 549–602, 669–712.
[10] T.C. Powers, Physical properties of cement paste, 4th, ISCC 1 (1960) 577–613.
[11] S. Igarashi, M. Kawamura, A. Watanabe, Analysis of cement pastes and mortars by combination of backscatter-based SEM image analysis and calculation based upon the Powers model, Cem. Concr. Compos. 26 (2004) 977–985.
[12] S. Diamond, M.E. Leeman, Pore size distributions in hardened cement paste by SEM image analysis, Mater. Res. Soc. Proc. 370 (1995) 217–226.
[13] E. Revertegat, C. Richet, P. Gégout, Effect of pH on the durability of cement pastes, Cem. Concr. Res. 22 (1992) 259–272.
[14] K. Yasuda, K. Yokozeki, Y. Kawata, Y. Yoshizawa, Physical and transportation properties of concrete due to calcium leaching (in Japanese), Cem. Sci. Concr. Technol. 56 (2002) 492–498.
[15] S. Bejaoui, B. Bary, Modeling of the link between microstructure and effective diffusivity of cement pastes using a simplified composite model, Cem. Conr. Res. 37 (2007) 469–480.
[16] J.V. Brakel, P.M. Heertjes, Analysis of diffusion in macroporous media in terms of a porosity, a tortuosity and a constrictivity factor, Int. J. Heat Mass Transfer 17 (1974) 1093–1103.
[17] J.H. Wang, Self-diffusion and structure of liquid water, J. Am. Chem. Soc. 73 (1951) 510–513.